J Mater Sci (2007) 42:2231–2235
DOI 10.1007/s10853-006-1319-6

4TH BRAZILIAN MRS MEETING

Scintillating properties of pure and doped BGO ceramics

Geane C. Santana · Ana Carolina S. de Mello · Mário E. G. Valerio · Zélia Soares Macedo

Received: 7 November 2005 / Accepted: 1 February 2006 / Published online: 8 March 2007

Abstract The ceramic processing and characterization of $Bi_4Ge_3O_{12}$ pure and doped with Eu^{3+} and Nd^{3+} was performed in order to investigate its potential use in radiation detector devices. Single phase $Bi_4Ge_3O_{12}$ in pure state and containing 1% of the dopands Nd^{3+} and Eu^{3+} were produced via a solid state route and their photoluminescent and radioluminescent properties were investigated. When excited at 200–230 nm, pure BGO ceramics presented a wide photoluminescent band emission centered at 450 nm, assigned to the Bi^{3+} internal transitions. For the doped samples under the same excitation, this wide band was superposed by the emission peaks of the rare earth dopands, at around 600 nm for BGO:Eu^{3+} and at 350 nm, 430 and 600 nm for BGO:Nd^{3+}. Radioluminescence measurements presented similar results and allowed the determination of the light output efficiency of the three scintillators. The values determined were 4×10^3 photons/MeV for BGO:Nd and 5.9×10^3 photons/MeV for BGO:Eu, which are higher than the value 3.9×10^3 photons/MeV determined previously for the pure ceramic. A selective sensibility of the BGO:Eu ceramics to the nature and energy of the radiation, which is not observed in pure samples, was also presented and discussed.

G. C. Santana · Z. S. Macedo (✉)
Grupo de Materiais Cerâmicos Avançados, Departamento de Física, Universidade Federal de Sergipe, Campus Universitário, 49, 100-000, Sao Cristovao, SE, Brazil
e-mail: zmacedo@fisica.ufs.br

A. C. S. de Mello · M. E. G. Valerio
Laboratório de Preparação e Caracterização de Materiais, Departamento de Física, Universidade Federal de Sergipe, Campus Universitário, 49, 100-000, Sao Cristovao, SE, Brazil

Introduction

Bismuth Germanate ($Bi_4Ge_3O_{12}$-BGO) have been the focus of several studies due to the interest in scintillator materials. It has a wide variety of applications in medicine and high energy physics [1, 2], and is often used in the single crystalline form.

Due to the difficulty to produce good quality large single crystals, there is a general search for the substitution of these materials by ceramics in many areas where scintillators are applied. In fact, scintillator ceramics have already some applications as radiation detectors [3, 4].

The growth of BGO single crystals is widely reported in the literature (see for example [5–7]) but there are only some few references concerning the synthesis of BGO ceramics [3, 8]. The advantages of using ceramics instead of single crystals are the homogeneous distribution of dopands, high output in mass production and the facility to conform ceramics in a large variety of shapes and sizes so improving the scintillator production process and usability.

In doped BGO, the trivalent cationic dopands are expected to occupy the Bi^{3+} site [9]. The doping of BGO single crystals with rare earth elements has been studied aiming the increase of the light output, and in some cases these additives also reduced the radiation damage [10, 11]. The present work reports the production and characterization of BGO scintillators doped with the rare earth elements Eu and Nd. The ceramic processing and structural characterization, as well as the photo and radioluminescence of these materials, are presented and discussed. The light output of these scintillators is compared with the efficiency of other crystalline and ceramic materials.

Experimental

The $Bi_4Ge_3O_{12}$ single phase powder was obtained by solid-state reaction. The precursor oxides used in stoichiometric proportion were Bi_2O_3 and GeO_2 (Alfa Aesar, 4N). These oxides were ball-milled for 80 h in plastic recipients containing the powders, zirconia balls and isopropyl alcohol in the volumetric proportion of 10:60:30. The as-dried material was calcined at 800 °C for 8 h in alumina crucible in an open atmosphere furnace. After the calcination, the powder was milled again for 48 h, mixed to a binder solution of polyvinyl alcohol and conformed by uniaxial pressing under 20 MPa in pellets with 6 mm in diameter and 2 mm in thickness. The ceramic bodies were then sintered at 840 °C (10 h) and reached a relative density of 97±1%. For the preparation of the 1 mol% doped samples $Bi_{3.96}Eu_{0.04}Ge_3O_{12}$ and $Bi_{3.96}Nd_{0.04}Ge_3O_{12}$ (hereafter called BGO:Eu and BGO:Nd) appropriated amounts of the precursors Eu_2O_3 (Alpha Aesar, 3N) and Nd_2O_3 (Aldrich, 3N) were added before the first milling.

The structural analysis of the calcined powders and sintered ceramics was made by X-ray diffraction (XRD - Rigaku DMAX 2000/PC) using CuKα radiation in continuous scanning mode, with scanning speed of 2°/min in the 2θ range from 10° to 80°.

Before the luminescence characterization the ceramic disks were polished to a thickness of ~0.4 mm with silicon carbide and alumina powder. After that, the samples were cleaned in an ultrasonic bath in acetone. The emission and excitation photoluminescence (PL) spectra were acquired at room temperature using a ISS/PC1 spectrofluorimeter with resolution of 4 nm for the excitation and 2 nm for the emission spectra. A 300W Xenon lamp was used as the excitation source. In the measurements of PL emission under excitation above the BGO band gap, two different wavelengths were used (200 and 230 nm) to avoid second harmonic emissions.

During the radioluminescence (RL) measurements, the samples were irradiated with a $^{90}Sr/^{90}Y$ β-rays source and the emitted light during the irradiation was detected using a Hamamatsu R928 photomultiplier tube. The current measured by the PMT was registered using a Keithley 6517 electrometer connected to a PC. The PMT and the β-rays source were positioned to form an angle of 90° between the irradiation beam and light detection. The dose rate measured at the sample position was about 0.2 Gy/min. For the measurements of the RL spectra from 200 nm to 800 nm, a monochromator (FUNBEC – Unicrom 100) with typical spectral bandwidth of 10 nm, was employed. The spectral intensities were normalized by the superficial area of the samples.

Results

Figure 1 presents the XRD patterns of the calcined powders and sintered ceramics of all the samples produced. It can be observed that the calcined powder presented the predominant phase $Bi_4Ge_3O_{12}$, and a very small amount of the phase $Bi_{12}GeO_{20}$. For the sintered ceramics only the crystalline phase $Bi_4Ge_3O_{12}$ was detected in the XRD patterns. In a previous work [12], it was observed that a very small amount of a liquid phase was formed in the grain boundaries during the sintering at 840 °C. This phase is probably $Bi_{12}GeO_{20}$, which melts at 780 °C and is possibly frozen in an amorphous structure, not detected by XRD.

Figure 2 presents the photoluminescence curve of BGO:Nd measured in the excitation mode for a emission wavelength of 598 nm. Two excitation bands were observed at 350 nm (3.6 eV) and 398 nm (3.1 eV). Both are below the BGO band gap (260 nm, 4.8 eV) [13, 14] and correspond to typical transitions of the dopand Nd^{3+} [15], as indicated in the graph.

Figure 3 presents the photoluminescence curve of BGO:Nd excited at 350 nm ($^4I_{9/2} \rightarrow {}^4D_{5/2} + {}^4D_{1/2} + {}^2I_{11/2}$ transitions Nd^{3+}). Only the typical emission of Nd^{3+} centered at 598 nm was registered under these conditions [16]. This same emission was also observed

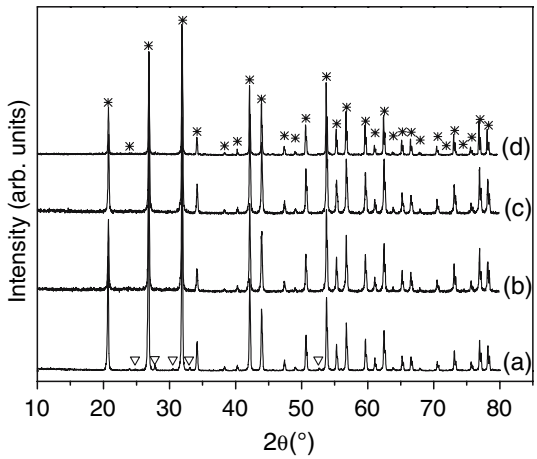

Fig. 1 XRD patterns of the pure BGO calcined powders (**a**) and sintered ceramics: (**b**) pure BGO, (**c**) BGO:Nd and (c) BGO:Eu. The diffraction peaks were indexed using JCPDS pattern references for $Bi_4Ge_3O_{12}$ (*) and $Bi_{12}GeO_{20}$ (∇)

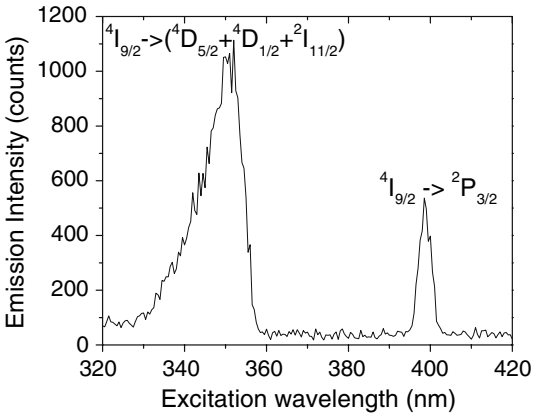

Fig. 2 Photoluminescence of BGO:Nd measured in the excitation mode with a emission wavelength of 598 nm ($^4G_{5/2} \rightarrow {}^4I_{9/2}$)

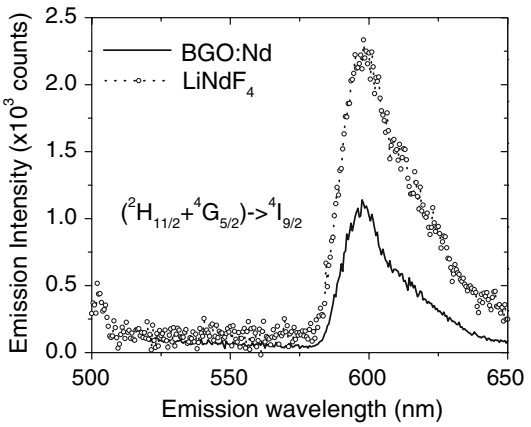

Fig. 3 Photoluminescence spectra of BGO:Nd and $LiNdF_4$ excited at 350 nm

in other materials containing Nd^{3+}, such as $LiNdF_4$ also presented in Fig. 3 for comparison purposes.

Similar result was observed for BGO:Eu. The photoluminescent emission of Eu^{3+} doped BGO ceramics excited under 410 nm (3.0 eV) is presented in Fig. 4. This excitation energy is below the BGO band gap (4.8 eV at room temperature [13, 14]) and corresponds to the transition $^7F_0 \rightarrow {}^5D_3$ of Eu^{3+} [17]. One can observe in this graph the typical emission bands of Eu^{3+} ion with the correspondent transitions indicated for each band.

The photoluminescence behavior of the doped ceramics assumed a completely different profile when the samples were irradiated with energies above the band gap, as it can be observed if Fig. 5. Exciting the pure and doped BGO ceramics under 200–230 nm produced an intrinsic emission similar to that reported for other materials where bismuth is present as a dilute activator ion, and assigned to $^3P_1 \rightarrow {}^1S_0$ transitions of Bi^{3+} [14]. For the doped ceramics, the PL emission

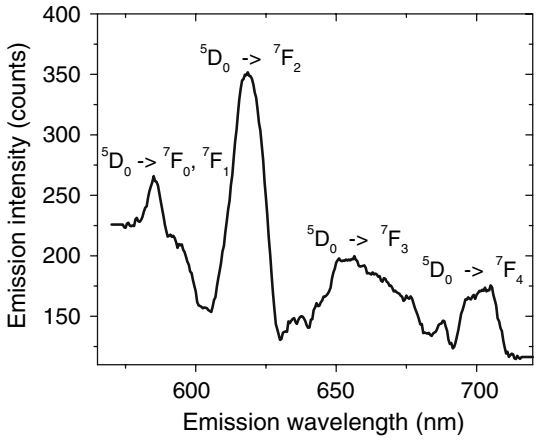

Fig. 4 Photoluminescence spectrum of BGO:Eu excited at 410 nm ($^7F_0 \rightarrow {}^5D_3$)

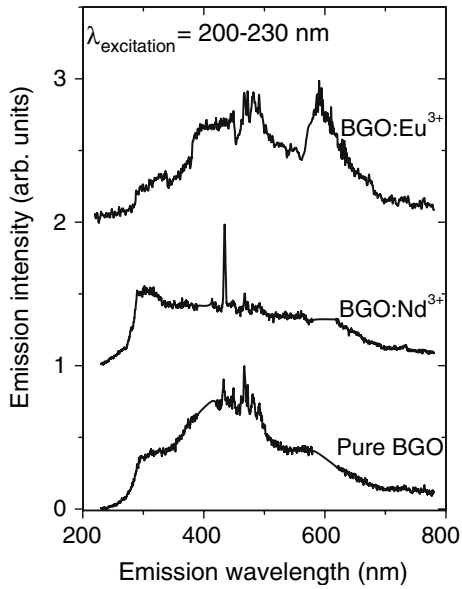

Fig. 5 Photoluminescence spectra of pure and doped BGO, excited at 200–230 nm

spectra presented the same band observed for pure BGO, superposed by the emission peaks of the rare earth dopands. For BGO:Eu the emission peak observed at around 600 nm correspond to the Eu^{3+} emission at 615 nm presented in Fig. 4. Comparing the pure and BGO:Nd spectra in Fig. 5, it can be observed in this latter that the intensities at the wavelength intervals from 280 to 330nm and 580 to 670 nm were enhanced relative to the region 350–500 nm, and that a sharp emission peak arose at 430 nm. The emissions at 350, 430 and 600 nm can be assigned to the same Nd^{3+} internal transitions presented in Figs. 2 and 3.

Radioluminescence (RL) measurements were performed in order to determine the intensity and

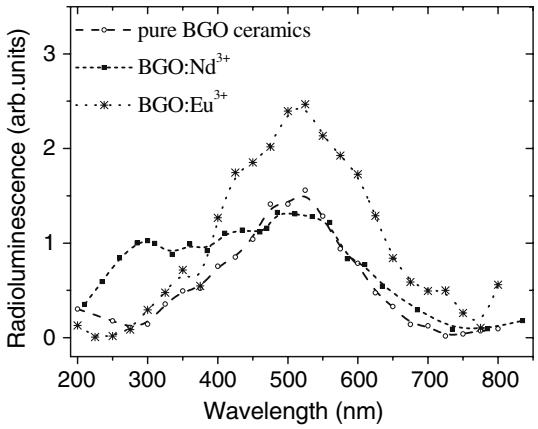

Fig. 6 RL spectra of the ceramics under irradiation with β-rays from $^{90}Sr/^{90}Y$ (700 ± 300 keV)

wavelength distribution of light output of the doped samples, compared to the pure BGO ceramics. Figure 6 presents the RL spectra of the ceramics under irradiation with β-rays. Due the lower resolution of the monochromator (10 nm for these measurements) the RL peaks are less defined than that presented in PL results. Nevertheless, the normalized intensities allow a direct comparison of the light output efficiencies.

Basically the same wavelength distributions were observed in RL emission excited by β-rays and PL spectra with excitation wavelength at 200–230 nm. In all the cases studied, doped samples presented the large radioluminescent band due to BGO matrix plus the typical rare earth emissions, resulting in higher efficiency for the radiation to light conversion. A possible explanation is that part of the energy that would generate non-radiative transitions in the pure samples is now being transferred to the excited levels of the dopands, which decays radiatively thus enhancing the overall light output of the scintillator.

The RL data presented in this work for BGO:Eu irradiated with β-rays (700 keV, with a 300 keV bandwidth) are significantly different from [11], which reports that under irradiation with 35 keV X-rays, the radioluminescence BGO:Eu of is governed by the optical transitions of the Eu^{3+} ion. On the other hand, the RL spectra of pure BGO excited with β-rays of 700 keV (present work) or X-rays of 35 keV [11] have the same wavelength distribution. This result reveals a selective sensibility of the BGO:Eu to the energy and/or radiation type that is not observed for the pure samples. This selectivity is probably related to the fact that X-ray energy at 35 keV is rather near the absorption K-edge of Europium [18], whereas the high energy of β-radiation is absorbed preferentially by the heavy Bi^{3+} ions. For practical purposes, BGO:Eu showed to be more suitable than pure ceramics for application in systems which requires energy resolution.

The light output of each scintillator can be obtained from the integration of its RL spectrum. The area under the curves of Fig. 6 obeys the proportion 1:1.13:1.5 for pure BGO, BGO:Nd and BGO:Eu, respectively. Considering that the value of pure BGO ceramics is 3.9×10^3 photons/MeV [3], a direct calculation leads one to the values 4.4×10^3 photons/MeV for BGO:Nd and 5.9×10^3 photons/MeV for BGO:Eu. These efficiencies are higher than the light output from CeF_3 single crystal (4×10^3 photons/MeV) and comparable to $BaHfO_3$:Ce ceramic (6×10^3 photons/MeV). Besides, the light output of BGO:Eu represents 67% of the efficiency of the single crystalline pure BGO [3, 19].

Conclusions

The ceramic processing and characterization by photo and radioluminescence of rare earth doped BGO were presented and discussed in the present work. The sintered ceramics presented relative density equal to 97%, with no spurious crystalline phase detected by XRD technique.

For doped ceramics it was verified that the dopands act as activators of the scintillating properties, creating new luminescent centers in the material. When excited above the BGO band gap the doped ceramics presented the typical BGO emission superposed by the emission peaks of the rare earth dopands. For the excitation below the band gap, the emission peaks corresponded to the rare earth transitions, which were not significantly modified by the crystalline matrix.

The Eu^{3+} doped samples presented a better energy resolution than the pure BGO, and this feature is very suitable for application in systems where energy discrimination is desirable, as for example high energy calorimeters. Furthermore, both BGO:Eu and BGO:Nd presented higher efficiency than the pure BGO ceramic scintillator. A comprehensive study of the dependency between the scintillator properties and the dopand concentration is currently being developed in our laboratory.

Acknowledgements The authors wish to acknowledge the financial support from FINEP, CNPq, FAPESP, CAPES and FAP-SE, Brazilian funding agencies.

References

1. Classe JM, Fiche M, Rousseau C, Sagan C, Dravet F, Pioud R, Lisbona A, Ferrer L, Campion L, Resche I, Curtet C (2005) J Nucl Med 46(3):395
2. Auffray E, Cavallari F, Lebeau M, Lecoq P, Schneegans M, Sempere-Roldan P (2002) NIM A 486:22
3. Macedo ZS, Silva RS, Valerio MEG, Hernandes AC (2003) NIM B 218:153
4. Greskovich C, Duclos S (1997) Ann Rev Mat Sci 27:69
5. Borovlev YA, Ivannikova NV, Shlegel VN, Vasiliev YV, Gusev VA (2001) J Crist Growth 229(1):305
6. Vaithianathan V, Kumaragurubaran S, Santhanaraghavan P, Muralidhar N, Kumar R, Sinha AK, Ramasamy P, Nagarajan T (2002) Mat Chem Phys 74(2):121
7. Macedo ZS, Martinez AL, Hernandes AC (2003) Mat Res 6(4):577
8. Macedo ZS, Hernandes AC (2002) J Am Ceram Soc 85(7):1870
9. Jazmati AK, Townsend PD (2000) NIM B 166(67):597
10. Shim JB, Yoshikawa A, Bensalah A, Fukuda T, Solovieva N, Nikl M, Rosetta E, Vedda A, Yoon DH (2003) J Appl Phys 93(9):5131
11. Shim JB, Yoshikawa A, Nikl M, Vedda A, Fukuda T (2003) Opt Mat 24:285
12. Macedo ZS, Silva RS, Martinez AL, Valerio MEG, Hernandes AC (2004) J Am Ceram Soc 87(6):1076
13. Rivas-Silva JF, Berrondo M (1998) J Phys Chem Solids 59(9):1627
14. Weber MJ, Monchamp RR (1973) J Appl Phys 44:5495
15. Kaminskii AA (1996) In Crystalline lasers: physical process and operation schemes. Taylor & Francis, Oxford, p 274
16. Ju JJ, Kwon TY, Kim HK, Kim JH, Kim SC, Cha M, Yun SI (1996) Mat Lett 29:13
17. Tsuboi T, Seo HJ, Moon BK, Kim JH (1999) Physica B 270:45
18. Elam WT, Ravel BD, Sieber JR (2002) Radiat Phys Chem 63:121
19. Blasse G (1994) Chem Mater 6:1465